Design and Optimization of a Dielectric-gas-based Single-phase Electrostatic Motor

Nannan Zhao
School of Mechanical and Electrical Engineering
Xi'an University of Architecture and Technology
Xi'an, China
znn5838@sina.com

Fei Lu, Hua Zhang, Chris Mi
Department of Electrical and Computer Engineering
San Diego State University
San Diego, USA
cmi@sdsu.edu

***Abstract*—Electrostatic motor can work as a supplement to the electromagnetic motor due to its simple structure, low cost, light weight, and high efficiency. Increasing the applied voltage under ultra-high vacuum (UHV) condition and using dielectric liquid with high relative permittivity are two approaches to increase its torque and make electrostatic motors competitive with the electromagnetic ones. This paper presents a dielectric-gas-based single-phase electrostatic motor with simplified construction. 3-D finite element analysis (FEA) simulation and optimization process of the electrostatic motor is performed and an electrostatic motor with a torque of 0.25 Nm and power of 50 W is designed. 3-D printing is used to build a prototype machine to eliminate the process of mould manufacture and achieve a weight reduction. Predicted capacitance of machine is compared with measured result and good agreement is achieved.**

Keywords—capacitance; electrostatic motor; dielectric; 3-D printing.

I. INTRODUCTION

Electrostatic field has many practical uses, e.g. capacitive power transfer utilizing electrostatic field can realize 150 mm wireless power transmission at high efficiency [1] [2]. Electrostatic motors are electromechanical devices utilizing electrostatic force generated between electrodes. Due to its simple structure, low cost, light weight and high efficiency, electrostatic motor can work as a supplement to the electromagnetic motor, especially in the applications under high temperature conditions or sensitive to magnetic fields. Such a synergistic is known as an electromagnetic field, and is the phenomenon that makes wireless communications, broadcasting, and control systems possible.

Generally, the energy density of electrostatics is much lower than that of electromagnetics in macro scale. However, electric field strength between electrodes increases rapidly with the decrease of distance, producing comparative electrostatic force. Nowadays, electrostatic motors, especially the variable elastance electrostatic motors have been widely used in micro-electro-mechanical-systems (MEMS) [3] [4]. The main drawback of the electrostatic motor the restricts its development is its relatively low value of torque, which can be improved by increasing the applied voltage under UHV condition or using dielectric liquid with high relative permittivity [5].

Progressive research work has been done in the dielectric-liquid-filled electrostatic motor. From reference [5-10], evaluation of dielectric fluids, the nature of electrostatic torque production, axial-peg-style motor topology and optimization design, capacitance and torque calculations and measurement, and 3-D printing manufacture technique are discussed. A fluid-filled electrostatic rotating machine, comparable to the fractional horsepower class induction machine, is constructed, indicating the potential use of electrostatic machines in fluid-filled applications.

The UHV approach has been employed by [11] [12]. Sensors are attached to detect the relative position between the electrodes on the stator and rotor side. Voltages of different polarities, switched according to pre-determined timing, are applied to the electrodes on the rotor side in order to generate constant driven torque between the stator and the rotor, resulting in an electrostatic motor in a high, clean vacuum with a voltage from 1 to 100 kV, a maximum speed of 10,000 rpm, a maximum torque of 0.1 Nm, a power of 100 W, and an efficiency >95%.

There are two contributions compared with previous works. Firstly, compared with previous work [5-12], two potentials of the presented single-phase electrostatic motor are distributed on two stators respectively, thus stator plate is no need to be insulated for different potentials, which simplifies the construction and reduces the manufacture complexity. Secondly, compared with previous liquid-filled work [5-10], this paper presents a dielectric-gas-based electrostatic motor, indicating the potential use of electrostatic machines in dielectric gas applications for low torque, low power and high speed applications.

II. MOTER TOPOLOGY AND DESIGN

Electrostatic motors are devices utilizing electrostatic force generated between electrodes. When power is applied to the stator electrodes, the rotor's electrical elastance creates a force that attempts to align the rotor electrodes with the nearest stator electrodes to minimize the elastance. Compared with

This work was supported by the Scientific Research Program through the Shaanxi Provincial Education Department under Program 2016JK1427.

electromagnetic motor, electrostatic motor is constructed of dielectric and electrode, eliminating the costly winding, permanent magnet and lamination core, thus the manufacture complexity and the cost of electrostatic machine can be reduced.

The proposed electrostatic motor has two stators and a rotor. The stators and rotor, fitted with concentric rows of interdigitated round electrodes on them, are opposed to each other in an axial direction. Assembly drawing of the electrostatic motor is shown in Figure 1. The force between the rotor and stator electrodes can be derived from the term of Lorentz Force contributed by electric fields. Considering the dynamic process of the rotor rotation and the interaction between the rotor and stator electrodes, torque T and capacitance C generated between the rotor and two stators can be expressed as:

$$T = V^2 \frac{\mathrm{d}}{\mathrm{d}x} C(x) = V^2 \frac{C_{stator1-rotor}(x) - C_{stator2-rotor}(x)}{\Delta x} \quad (1)$$

$$C(x) = N \frac{\varepsilon_0 \varepsilon_r s}{\mathrm{d}(x)} \quad (2)$$

where V is the applied voltage, x is the relative distance between the rotor and the stator, N is the number of electrodes of the rotor and the stator, s is the effective interaction area between the rotor and stator electrodes. According to equation (1), the design emphasis lies on that the variation of the coupling capacitance with distance should be large enough to supply adequate torque.

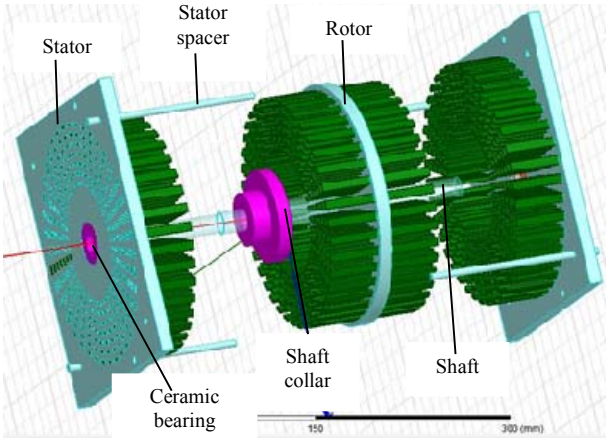

Figure 1: Assembly drawing of presented electrostatic motor

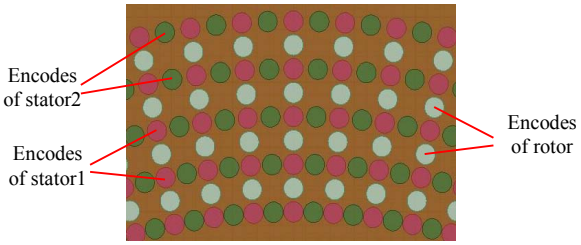

Figure 2: Topology arrangement of electrostatics.

The topology of two stators are identical with 180 electrical degrees difference in the spatial location, as shown in Figure 2, which ensures a maximum capacitance variation. The main parameters of the motor with round electrodes are shown in Table I. The performance of topologies with rectangle electrode shape will be compared in part III. 3-D FEA models of motor are built in Maxwell. The capacitances between the stator and the rotor with different pole combination (stator poles/rotor poles of 96/96; 96/64; 96/48; respectively), as shown in Figure 3, are compared to obtain the rule on how the capacitances change with distance.

TABLE I. PARAMETERS OF MOTOR

Parameters	Round electrode	Rectangle electrode
Number of rows-stator	5	7
Number of rows-rotor	4	6
Electrode diameter/thickness	3.2 mm	3 mm
Electrode overlapping length	25 mm	35 mm
Minimum gap	0.5 mm	1 mm
Row-to-row space	3.7 mm	4 mm
Stator first row radius	100 mm	50 mm
Stator plate outer radius	165 mm	110 mm

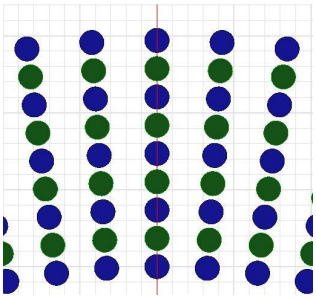

(a) stator poles/rotor poles of 96/96

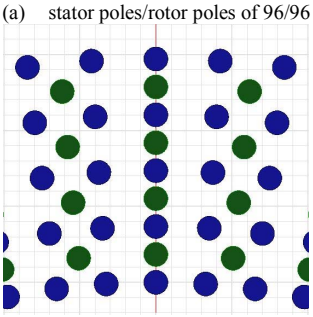

(b) stator poles/rotor poles of 96/64

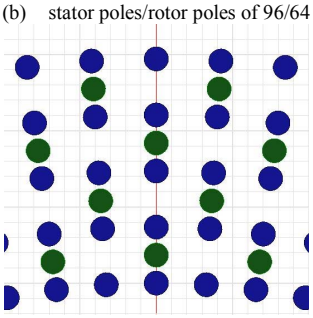

(c) stator poles/rotor poles of 96/48

Figure 3: Electrodes distribution of stator 1 and rotor with different pole combination.

Capacitances between the rotor and the stator 2 are 180 degree shifted in phase position compared with capacitance between rotor and stator 1. Therefore, the capacitances between the rotor and the stator 2 of 96/64 topology and 96/48 topology are not shown in Figure 4. As can be seen, the amplitudes of capacitances of the 96/96 topology are higher than those of the 96/64 topology and the 96/48 topology due to more electrode number. The capacitances of three topologies all reach maximum at 0° position. The capacitances of the 96/96 topology reaches minimum at 1.875° position, while the capacitances of the 96/64 topology reaches minimum at 0.9375° position, causing the variation of capacitance of 96/96 topology is higher than that of 96/64 topology. Therefore, the rule can be derived that the number of electrodes influences the amplitude of the capacitance, and that the distance over which the maximum and minimum capacitance occur influences the variation of the capacitance.

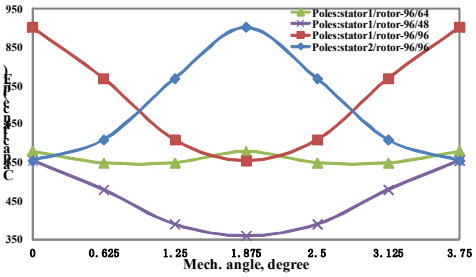

Figure 4: Capacitances between stator and rotor with different pole combination.

III. Motor Optimization

The prototype machine is downsized to improve the power density and save the material. The stator plate outer radius decreased from 165mm to 110mm, while the variation of capacitance is also guaranteed. Optimum design is employed by comparing the capacitance of different topologies (electrode number/shape/overlapping length/span angle α of 60/round/25mm/N/A, 60/rectangle/35 mm/3°, 48/rectangle/35 mm/3°, 40/rectangle/35 mm/4.5°, respectively). Figure 5 shows the topology of a rotor and a stator with rectangle electrostatics of 40/ rectangle /35 mm/4.5°. Rectangle electrodes are modified with round corners to avoid sharp edges resulting in breakdown event. Capacitances between the stator 1 and the rotor of different topologies are shown in Figure 6, of which the capacitance characteristic of topology with electrode number/shape/overlapping length/span angle α of 40/ rectangle /35 mm/4.5° is the best. Compared with previous capacitance characteristic of the 96/round/25mm/N/A topology, although the size of the motor and the electrode number are decreased and the minimum gap is enlarged, the optimized capacitance characteristic can be obtained by improving electrode shape from round to rectangle and increasing electrode overlapping length and span angle to increase the effective interaction area between the rotor electrode and stator electrode. Subsequently, torque density is improved.

The parameters of the prototype motor with rectangle electrode are established based on the 40/rectangle/35 mm/4.5°

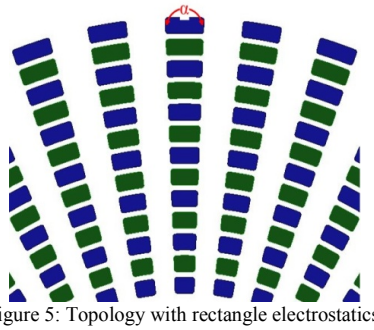

Figure 5: Topology with rectangle electrostatics.

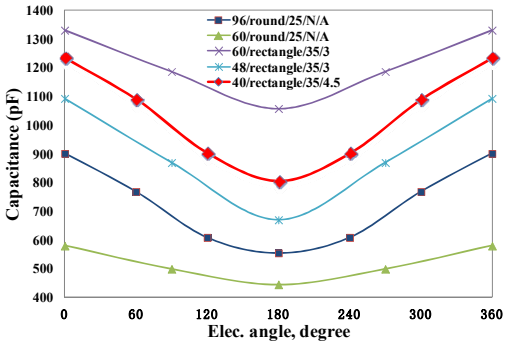

Figure 6: Capacitances between stator 1 and rotor of different topologies.

topology, as shown in Table I. Based on the simulated result of capacitance and equation (1), torque can be derived in the level of:

$$T = V^2 \frac{\mathrm{d}}{\mathrm{d}x} C(x) = 4\times10^6 \times \frac{400\times10^{-12}}{6.28\times10^{-3}} = 0.25\mathrm{Nm} \qquad (3)$$

where the voltage supplied is assumed to be at 2×103 V.

speed of motor:

$$n = \frac{60f}{P} = \frac{60\times5000}{40} = 7500\mathrm{rpm} \qquad (4)$$

where the frequency supplied is assumed to be at 5×103 Hz.

power of motor:

$$P = \omega C V^2 = 2\times3.14\times5000\times400\times10^{-12}\times4\times10^6 = 50\mathrm{W} \qquad (5)$$

as can be seen, torque and power can be increased by increasing the supplied voltage and frequency. However, a special method, e.g. UHV or insulating gas conditions, should be employed to avoid the breakdown event. Besides, the windage loss and the mechanical strength should be considered.

IV. Prototype Machine Construction and Test

3-D printing is a process of creating three dimensional objects using additive processes. Unlike material removed from a stock in the conventional machining process, 3-D printing builds a three-dimensional object from computer-aided design (CAD) model by successively adding material layer by layer. Thus, objects of almost any shape or geometry can be produced using 3-D printing. In order to eliminate the process of mould manufacture, 3-D printing is used to build the

prototype machine in plastic and nickel is plated on surface to make the prototype machine conductive. 3-D printed rotor and stator using PLA plastic, as well as prototype machine assembled, are shown in Figure 7.

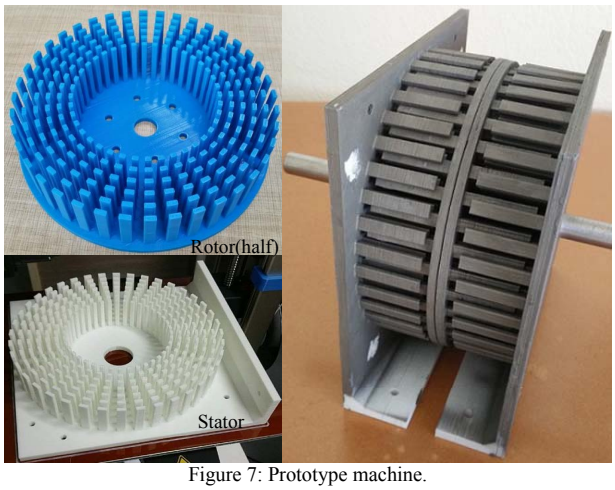

Figure 7: Prototype machine.

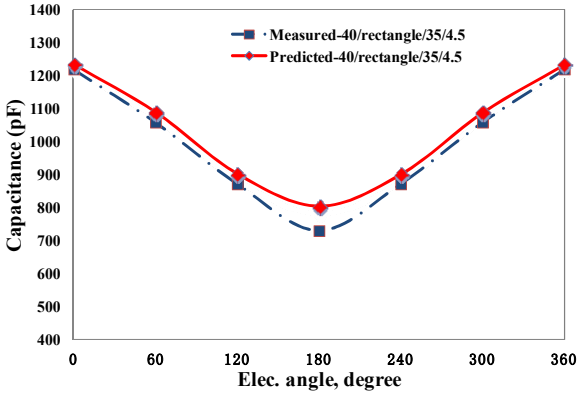

Figure 8: Comparison of capacitance result and measured data.

Comparison of capacitance result and measured data is shown in Figure 8. As can be seen, good agreement is achieved. The slightly difference between the measured result and the predicted result may be due to the errors in manufacture technology. The comparison result validates the design and optimization process of the presented dielectric-gas-based single-phase electrostatic motor

V. CONCLUSIONS AND FUTURE WORK

In this paper, a dielectric-gas-based single-phase electrostatic motor is presented. Compared with previous liquid-filled and UHV works, two potentials of the single-phase electrostatic motor are distributed on two stators respectively, thus stator plate is no need to be insulated for different potentials, which simplifies the construction and reduces the manufacture complexity. Optimization design is performed and an electrostatic motor with a torque of 0.25 Nm, and 50 W power is obtained. Achievable 3-D printing is used to build the prototype machine to eliminate the process of mould manufacture and achieve a weight reduction. Predicted capacitance of machine is compared with measured result and good agreement is achieved. Future work includes drive design and performance testing of the electrostatic motor.

REFERENCES

[1] F. Lu, H. Zhang, H. Hofmann, C. Mi, "An Inductive and Capacitive Combined Wireless Power Transfer System," *IEEE Trans. Power Electron.,* vol. 31, no. 12, pp. 8471-8482, Dec. 2016.

[2] F. Lu, H. Zhang, H. Hofmann, C. Mi, "A Double-Sided LCLC-Compensated Capacitive Power Transfer System for Electric Vehicle Charging," *IEEE Trans. Power Electron.,* vol. 30, no. 11, pp. 6011-6014, Nov. 2015.

[3] B. Q. Sun, F. T. Han, L. L. Li, and Q. P. Wu, "Rotation Control and Characterization of High-Speed Variable-Capacitance Micromotor Supported on Electrostatic Bearing," *IEEE Trans. Ind. Electron.,* vol. 63, no. 7, pp. 4336–4345, JUL. 2016.

[4] A. Ketabi and M.J. Navardi, "Optimization of variable-capacitance micromotor using genetic algorithm," *J. Microelectromech Syst.*, vol. 20, no. 2, pp. 497-504, Feb. 2011.

[5] B. Ge and D. C. Ludois, "Design Concepts for a Fluid-Filled Three-Phase Axial-Peg-Style Electrostatic Rotating Machine Utilizing Variable Elastance," *IEEE Trans. Ind. Appl.*, vol. 52, no. 3, pp. 2156–2166, May 2016.

[6] B. Ge and D. C. Ludois, "Dielectric Liquids for Enhanced Field Force in Macro Scale Direct Drive Electrostatic Actuators and Rotating Machinery," *IEEE Trans. Dielectr. Electr. Insul.,* vol. 23, no. 4, pp. 1924–1934, Aug. 2016.

[7] B. Ge, D. C. Ludois, and A. N. Ghule, "A 3D printed fluid filled variable elastance electrostatic machine optimized with conformal mapping," in *IEEE 2016 Energy Conversion Congress and Exposition (ECCE)*, 2016, pp. 1–8.

[8] B. Ge and D. C. Ludois, "A 1-phase 48-pole axial peg style electrostatic rotating machine utilizing variable elastance," in *IEEE 2015 International Electric Machines Drives Conference (IEMDC)*, 2015, pp. 604–610.

[9] B. Ge and D. C. Ludois, "Evaluation of dielectric fluids for macro-scale electrostatic actuators and machinery," in *IEEE 2014 Energy Conversion Congress and Exposition (ECCE)*, 2014, pp. 1457–1464.

[10] R. O'Donnell, N. Schofield, A. C. Smith, and J. Cullen, "Design concepts for high-voltage variable-capacitance DC generators," *IEEE Trans. Ind. Appl.*, vol. 45, no. 5, pp. 1778–1784, Sep./Oct. 2009.

[11] T. Sashida, "Electrostatic motor," U.S. Patent 8278797 B2, Oct. 2, 2012.

[12] "Technology: High Power Electrostatic Motor – SHINSEI CORPORATION." [Online]. Available: http://www.shinsei-motor.com/English/techno/index.html.